Author Manuscript

Author Manuscript

Author Manuscript

Author Manuscript

HHS Public Access

Author manuscript

Leukemia. Author manuscript; available in PMC 2022 September 10.

Published in final edited form as:

Leukemia. 2022 May ; 36(5): 1313–1323. doi:10.1038/s41375-022-01536-x.

In Vivo Anti-Tumor Effect of PARP Inhibition in IDH1/2 Mutant MDS/AML Resistant to Targeted Inhibitors of Mutant IDH1/2

Rana Gbyli[1,*], **Yuanbin Song**[1,2,*,#], **Wei Liu**[1,*], **Yimeng Gao**[1,*], **Giulia Biancon**[1], **Namrata S Chandhok**[1,3], **Xiaman Wang**[1,4], **Xiaoying Fu**[1,5], **Amisha Patel**[1], **Ranjini Sundaram**[6], **Toma Tebaldi**[1], **Padmavathi Mamillapalli**[1], **Amer M Zeidan**[1], **Richard A. Flavell**[7,8], **Thomas Prebet**[1], **Ranjit S. Bindra**[6,9], **Stephanie Halene**[1,10,#]

[1]Section of Hematology, Department of Internal Medicine and Yale Comprehensive Cancer Center, Yale University School of Medicine, New Haven, CT, 06520, USA.

[2]Current affiliation: Department of Hematologic Oncology, Sun Yat-sen University Cancer Center, State Key Laboratory of Oncology in South China, Collaborative Innovation Center for Cancer Medicine, Guangzhou, 510062, China.

[3]Section of Hematology, Department of Internal Medicine, University of Miami, Coral Gables, FL, USA.

[4]Department of Hematology, the Second Affiliated Hospital of Xi'an Jiaotong University, Xi'an, P. R. of China.

[5]Department of Laboratory Medicine, Shenzhen Children's Hospital, Shenzhen, P. R. of China.

[6]Department of Therapeutic Radiology, Yale University, New Haven, CT, 06520, USA.

[7]Department of Immunobiology, Yale University School of Medicine, New Haven, CT, USA.

[8]Howard Hughes Medical Institute, Yale University, New Haven, Connecticut, USA.

[9]Department of Pathology, Yale University, New Haven, CT, 06520, USA.

[10]Yale Stem Cell Center and Yale RNA Center, Yale University School of Medicine, New Haven, CT, 06520, USA

Abstract

Treatment options for patients with relapsed/ refractory acute myeloid leukemia (AML) and myelodysplastic syndromes (MDS) are scarce. Recurring mutations, such as mutations in

Users may view, print, copy, and download text and data-mine the content in such documents, for the purposes of academic research, subject always to the full Conditions of use: https://www.springernature.com/gp/open-research/policies/accepted-manuscript-terms

[#]Co-corresponding authors **Corresponding Authors:** Yuanbin Song, M.D. Department of Hematologic Oncology, Sun Yat-sen University Cancer Center, State Key Laboratory of Oncology in South China, Collaborative Innovation Center for Cancer Medicine, 651 Dongfeng East Road, Guangzhou, China, 510062; Songyb@sysucc.org.cn, Stephanie Halene, M.D. Ph.D. Section of Hematology, Yale Cancer Center and Department of Internal Medicine, Yale University School of Medicine, 300 George St. 786E, P.O. Box 208073, New Haven, CT, 06520-8073, USA; Phone: 203 785-4144; stephanie.halene@yale.edu.

[*]Co-first authors

Author contributions

Conceptualization, S.H., R.S.B. and Y.S.; Methodology, S.H., R.G., and Y.S.; Investigation, Y.S., R.G., W.L., Y.G., G.B., X.W., X.F., N.C., R.S., A.P., T.T., and P.M.; Data analysis, Y.S., R.G. and S.H.; Validation, Y.S., R.G., and S.H.; Writing – Original Draft, S.H., R.G., Y.S.; Writing – Review & Editing, S.H., R.S.B., R.G., Y.S.; Funding Acquisition, S.H. and R.S.B.; Resources, R.G., A.P., A.M.Z., R.A.F. and T.P.; Project Administration, S.H. and R.S.B.; Supervision, S.H. and R.S.B.

Author Manuscript Author Manuscript Author Manuscript Author Manuscript

isocitrate dehydrogenase-1 and −2 (IDH1/2) are found in subsets of AML and MDS, are therapeutically targeted by mutant enzyme-specific small molecule inhibitors (IDH^mi). IDH mutations induce diverse metabolic and epigenetic changes that drive malignant transformation. IDH^mi alone are not curative and resistance commonly develops, underscoring the importance of alternate therapeutic options. We were first to report that IDH1/2 mutations induce a homologous recombination (HR) defect which confers sensitivity to poly (ADP)-ribose polymerase inhibitors (PARPi). Here, we show that the PARPi olaparib is effective against primary patient-derived IDH1/2-mutant AML/ MDS xeno-grafts (PDXs). Olaparib efficiently reduced overall engraftment and leukemia-initiating cell frequency as evident in serial transplantation assays in IDH1/2-mutant but not -wildtype AML/MDS PDXs. Importantly, we show that olaparib is effective in both IDH^mi-naïve and -resistant AML PDXs, critical given the high relapse and refractoriness rates to IDH^mi. Our pre-clinical studies provide a strong rationale for the translation of PARP inhibition to patients with IDH1/2-mutant AML/ MDS, providing an additional line of therapy for patients who do not respond to or relapse after targeted mutant IDH inhibition.

Introduction

The isocitrate dehydrogenase-1 and −2 (IDH1/2) genes encode key metabolic enzymes in the Krebs cycle that catalyze the reversible conversion of isocitrate to alpha-ketoglutarate (αKG) [1]. IDH1/2 mutations are found in approximately 20% of AML and in 4 to 12% of MDS [2, 3]. Somatic missense mutations in IDH1/2 occur within the catalytic sites at arginine residues R132 for IDH1 (the cytoplasmic isoform) and R140 or R172 for IDH2 (the mitochondrial isoform) [2–4]. IDH1/2 enzymes function as homodimers, and when mutated, acquire the neomorphic function as heterodimers to catalyze the conversion of αKG to 2hydroxyglutarate (2HG) [1]. 2HG is an oncometabolite that has been shown to promote leukemogenesis via the competitive inhibition of αKG-dependent dioxygenases involved in the regulation of DNA and histone methylation and other functions [5–8]. Given their important role in tumor initiation and progression, mutant IDH1/2 enzymes represent an attractive therapeutic target leading to the development of selective small molecule inhibitors [9]. Ivosidenib and enasidenib, inhibitors of mutant IDH1 and IDH2, respectively, have been approved in the treatment of adults with AML and MDS [10, 11], however, when given as single agents are not curative, with complete response (CR) rates and median overall survival (OS) ranging between 20–30% and ~8–12 months, respectively [12]. IDH^mi induce cell differentiation [2, 13] with persistence of the mutant IDH1/2 clones even in patients who achieve CR [14]. Resistance to IDH^mi is notable for either persistent or restored 2HG production [15–18].

We previously reported that mutant IDH1/2-induced 2HG accumulation induces a HR defect that confers sensitivity to PARPi [19]. Mechanistically, 2HG-induced inhibition of the lysine demethylase KDM4B results in aberrant hypermethylation of histone 3 lysine 9 (H3K9) at loci surrounding DNA breaks, masking the local H3K9 trimethylation signal essential for DNA double-strand break (DSB) repair via HR [20]. Tip60 and ATM fail to localize to DSBs, which results in impaired end-resection and recruitment of downstream HR factors. We identified similar oncogenic mechanisms secondary to TCA cycle gene mutations in fumarate hydratase and succinate dehydrogenase deficient cancers, highlighting

Author Manuscript Author Manuscript Author Manuscript Author Manuscript

the tumor agnostic nature of this “oncometabolite-induced BRCAness” and its potential as an exploitable vulnerability across different cancers [21] including leukemia and MDS. 2HG-induced HR deficiency renders cancer cells unable to resolve DSBs and sensitive to additional inhibition of single strand break (SSB) repair by PARPi [9, 19]. *In vivo* pre-clinical studies are necessary to bring novel concepts to the clinic and prove the validity of exploiting the 2HG-induced BRCAness defect with PARPi [19, 22, 23].

Here we show that mutant IDH1 and IDH2 confer sensitivity to PARPi *in vivo* not only in IDH^{m}i naïve but also in resistant MDS/AML. Using genetically matched patient-derived IDH1/2 mutant and wildtype MDS/AML PDX models in cytokine humanized immunodeficient mice that recapitulate the mutational heterogeneity of AML/MDS [24], we demonstrate that the PARP inhibitor olaparib significantly reduces MDS/AML engraftment and leukemia-initiating cell (LIC) frequency in IDH1/2 mutant but not wildtype MDS/AML. This sensitivity is maintained in IDH^{m}i resistant AML irrespective of co-occurring mutations. Our findings provide the rationale for the incorporation of PARPi into the treatment armamentarium for MDS/AML and the basis upon which to design combination therapies for relapsed/refractory and possibly treatment for naïve IDH1/2 mutant MDS/AML.

Materials and Methods

Primary patient samples

All patients’ PB and BM samples were obtained with donor’s written consent and accessed from the Yale hematology tissue bank. All human studies were approved by the Yale University Human Investigation Committee. Mononuclear cells were isolated using Ficoll-Paque separation (GE Healthcare, Cat#17–1440-03) and cryopreserved in fetal bovine serum (Gemini-Bioproducts, Cat#100–106) with 10% dimethyl sulfoxide.

Animal studies

All animal experiments were approved by and carried out in compliance with the Yale Institutional Animal Care and Use Committee protocols.

Primary murine AML model: FLT3$^{ITD/WT}$ IDH2$^{R140Q/WT}$ mice were a gift from Dr. Ross Levine’s lab and have been previously described [25]. Mx1Cre^{+} Flt3$^{ITD/WT}$ IDH2$^{R140Q/WT}$ mice were treated every other day with Polyinosinic: polycytidylic acid [poly (I:C)] (Calbiochem, Cat#528906) via intra-peritoneal (IP) injection at a dose of 20μg/g starting 4–6 weeks after birth. 6–9 months later, donor mice were euthanized and BM cells harvested from femurs and tibias, and lineage depleted using anti-mouse lineage cell detection cocktail antibody and BD IMag Streptavidin Particles Plus (BD Biosciences, Cat# 557812, RRID: AB_10050580).

MISTRG patient derived xenotransplantation (PDX) studies: MIS$^{h/h}$TRG mice (*CSF1*$^{h/h}$ *IL3/CSF2*$^{h/h}$ *SIRPA*$^{h/h}$ *THPO*$^{h/h}$ *Rag2*$^{-/-}$ *Il2rg*$^{-/-}$) were bred to MIS$^{m/m}$TRG mice (*CSF1*$^{h/h}$ *IL3/CSF2*$^{h/h}$ *Sirpa*$^{m/m}$ *THPO*$^{h/h}$ *Rag2*$^{-/-}$ *Il2rg*$^{-/-}$) to generate human cytokine homozygous and hSIRPA heterozygous mice (MIS$^{h/m}$TRG, labeled MISTRG throughout

Author Manuscript Author Manuscript Author Manuscript Author Manuscript

the study) [24, 26]. Mice were maintained on continuous treatment with enrofloxacin in the drinking water (0.27 mg/mL, Baytril, Bayer Healthcare). MISTRG mice have been deposited at the Jackson laboratory. IDH1/2 mutant and wild type AML patient samples were transplanted into newborn (3–5 days) MISTRG mice after irradiation twice with 150 cGy (XRAD 320, PXI X-Ray Systems) 4 hours apart. AML patient PB or BM mononuclear cells were incubated with anti-human CD3 antibody (clone Okt3, BioXCell, Cat# BE0001–2, RRID: AB_1107632) at 5 μg/100 μl for 30min prior to injection. Cells were injected intra-hepatically in a volume of 20 μL with a 22-gauge Hamilton needle and Hamilton syringe (Hamilton, Reno). Mice were analyzed at time points indicated via flowcytometry as previously described [24]. For secondary transplantation, cryopreserved BM cells from primary MISTRG recipient were thawed and depleted of murine cells via negative selection of murine $CD45^+$ and $Ter119^+$ cells by magnetic labeling with biotin-anti-mouse CD45 (clone 30-F11, Biolegend, Cat#103103, RRID: AB_312968) and biotin anti-mouse TER119 (clone TER-119, Biolegend, Cat#116204, RRID: AB_313705) and BD IMag Streptavidin Particles Plus (BD Biosciences, Cat# 557812, RRID: AB_10050580). Purified cells were incubated with anti-human CD3 antibody and injected intra-hepatically into MISTRG mice as described above. 8 to 12 weeks (AML) and 12 to 16 weeks (MDS) post transplantation, BM was aspirated from transplanted mice to quantitate human $CD45^+$ engraftment levels by flow cytometry and to assign mice to treatment groups based on equal engraftment levels. For tertiary transplantation to determine LIC frequency, equal numbers of $huCD45^+$ cells obtained from vehicle or drug treated mice were transplanted into newborn recipients, and analysis was performed at 16 weeks post transplantation.

Drug treatment

Olaparib (AZD2281) (Selleckchem, Cat#S1060) was dissolved in PBS containing 10% (w/v) 2-hydroxy-propyl-beta-cyclodextrin (Sigma) at a concentration of 20mg/ml. For *in vivo* studies, olaparib was administered IP at 100 mg/kg once daily. Enasidenib was purchased from LeadGen Labs, USA and dissolved in 0.5% methylcellulose and 0.2% Tween 80 in PBS at a concentration of 4 mg/ml and administered via oral gavage at 40 mg/kg once daily. 2-HG was measured in plasma before and after treatment with vehicle, enasidenib, or olaparib in triplicates with the D-2-Hydroxyglutarate (D2HG) assay kit (Biovision, Cat#K970–100, Sigma, Cat# MAK320–1KT) according to manufacturer's protocol.

Flow cytometric analysis of human cell engraftment in MISTRG mice

Engraftment of human $CD45^+$ cells and their subsets were determined by flow cytometry. In brief, cells were isolated from engrafted mice, blocked with human BD Fc block antibody (BD Biosciences, Cat#564219, RRID: AB_2728082) and mouse BD Fc block (2.4G2, BD Pharmingen, Cat#553141, RRID: AB_394656), and stained with combinations of antibodies purchased from Biolegend: Hematopoietic Stem and Progenitor Cell (HSPC) panel: APC/Cy7 mCD45 (30-F11, 1:300, Cat#103116, RRID: AB_312981), APC/Cy7 mTer119 (Ter-119, 1:300, Cat#116223, RRID: AB_2137788), BV510 hCD45 (HI30, 1:100, Cat#304036, RRID: AB_2561940), BV421 huCD38 (HIT2, 1:100, Cat#303526, RRID: AB_10983072), PE huCD34 (561, 1:100, Cat#343606, RRID:AB_1732008), PE/Cy7 huCD10 (HI10a, 1:100, Cat#312214, RRID: AB_2146548). Human cell engraftment panel:

Author Manuscript Author Manuscript Author Manuscript Author Manuscript

APC/Cy7 mCD45 (30-F11, 1:300), APC/Cy7 mTer119 (Ter-119, 1:300), BV510 hCD45 (HI30, 1:100), FITC huCD3 (OKT3, 1:100, Cat#317306, RRID: AB_571907), PE/Cy7 huCD19 (HIB19, 1:100, Cat#302216, RRID: AB_314246), APC huCD33 (WM53, 1:100, Cat#983902, RRID: AB_2810824), PE huCD34 (561, 1:100). Data were acquired with FACSDiva on an LSR Fortessa (BD Biosciences) equipped with 5 lasers and analyzed with FlowJo V10 software.

Histologic analysis

Tissues were fixed in BBC Biochemical B-PLUS FIX Fixative solution (Thermo Fisher Scientific, Cat#NC9496646) and embedded in paraffin. Femurs were decalcified with Formic Acid Bone Decalcifier (Decal Chemical, NY, USA). Paraffin blocks were sectioned at 4 μm and stained with hematoxylin and eosin (H&E) and antigen-specific antibodies by the Yale Clinical Pathology and Yale Pathology Tissue Services. Antibodies: human CD45, Leucocyte Common Antigen, (clone PD7/26+2B11, Dako, Cat#GA75161–2). Images were acquired using a Nikon Eclipse 80i microscope.

DNA cloning and cell culture

Site-directed mutagenesis to introduce the $IDH2^{Q316E}$ and $IDH2^{I319M}$ mutations was performed using the QuikChange II Site-Directed Mutagenesis Kit (Agilent Technologies, Cat#200521) with primers ($IDH2^{Q316E}$ Forward: CTATGACGGAGATGTGGAGTCAGACATCCTGGC; $IDH2^{Q316E}$ Reverse: GATACTGCCTCTACACCTCAGTCTGTAGGACCG; $IDH2^{I319M}$ Forward: AGATGTGCAGTCAGACATGCTGGCCCAGG; $IDH2^{I319M}$ Reverse: CCTGGGCCAGCATGTCTGACTGCACATCT). Wild type (WT) and mutant IDH2 were cloned into the LeGO-iC plasmid, a gift from Boris Fehse (Addgene plasmid, #27462) and verified by Sanger sequencing. Lentiviral particles were produced by co-transfection with transgene, VSVG and psPAX2 (gifts from Tannishtha Reya (Addgene plasmid # 14888 and #12260) in HEK293T cells (ATCC Cat# CRL-3216) using polyethylenimine transfection reagent (Polysciences Cat# 23966–2) followed by spin-concentration (Beckman, 27,000xg, 90min). Lineage depleted murine $Flt3^{ITD}IDH2^{R140Q}$ BM cells were pre-cultured with 8 μM Cyclosporine H (Sigma, SML1575) for 4 hours and then infected with viral particles via spinfection (1000xg at 25C for 1 hour) in StemSpan™ medium (Stem Cell Technologies) with addition of 8 μg/ml polybrene (Sigma) and recombinant murine cytokines (20 ng/ml Interleukin-3 (mIL-3, Cat#300–324P), 100 ng/ml Stem Cell Factor (mSCF, Cat#300–348P), 50 ng/ml Thrombopoietin (mTPO, Cat# 300–351P), 100 ng/mL Flt-3 Ligand (mFLT-3L, Cat#300–306P)) and 10% Penicillin-Streptomycin (Sigma). All cytokines were purchased from Gemini-Bioproducts. Cells were sorted for mCherry fluorescence 72 hours after transduction on a FACS Aria (BD Biosciences). Sorted cells were plated in methocult (StemCell Technologies Cat# M3434) in the presence of DMSO, enasidenib (50nM), or olaparib (1.25μM) in 35mm dishes in triplicates at a density of 1.2×10^4 cells per ml. Colonies were counted after 7 days and serially re-plated and re-counted.

Targeted next generation sequencing

Genomic DNA (gDNA) was extracted from BM (diagnosis, Y1597) or PB (relapse, Y2260) mononuclear cells using QIAGEN DNeasy Blood & Tissue kit according to manufacturer's

Author Manuscript Author Manuscript Author Manuscript Author Manuscript

instructions. Concentration and purity of the extracted gDNA were assessed using NanoDrop 1000 spectrophotometer (Thermo Scientific). During library preparation, IDT's xGen Acute Myeloid Leukemia Cancer Panel v1.0 (Integrated DNA Technologies) was used for the targeted enrichment of 264 genes associated with AML (11731 probes, 1.19 Mb of target regions from 6235 exons). Hybridization capture of DNA libraries and sequencing (Illumina HiSeq, paired-end 100bp) were performed at the Yale Center for Genome Analysis (YCGA). Raw FASTQ files were subjected to quality control through FastQC v0.11.5 [27]. Sequencing reads were then aligned to the human genome (GRCh38.p10) with Burrows-Wheeler Aligner (BWA-MEM, v0.7.15) using default parameters [28]. Duplicate reads were removed with Picard v2.9.0 (http://broadinstitute.github.io/picard/). The number of total aligned reads before and after duplicate removal was obtained using SAMtools [29] v1.5. Median coverage at each position in each enriched targeted region was calculated using BEDTools v2.27.1 [30]. Single-nucleotide variants (SNVs) and indels were detected with Genome Analysis Toolkit (GATK) v4.0.6.0 (https://github.com/broadinstitute/gatk) running Mutect2 [31] in tumor-only mode after base quality recalibration. Variants were annotated using ANNOVAR (2019Oct24) [32] and high-confidence variants were filtered as follows: exclusion of false positives (technical artifacts, germline variants and sequencing errors) through GATK4 filtering; exclusion of variants with synonymous or unknown effect; selection of deleterious variants (FATHMM-MKL prediction score) [33]; selection of variants annotated in COSMIC v90 [34]. This last filter was not applied to IDH2 variants to deeply explore regions potentially affected by PARPi treatment. All reported variants were visually inspected with the Integrative Genomics Viewer (IGV) [35].

Statistical analysis

Data was analyzed using Prism 8 (GraphPad Software, La Jolla, CA) with the use of paired Ratio t-test and unpaired Mann-Whitney U test as indicated. P value was considered significant at values less than 0.05, n.s. not significant, * statistically significant ($p<0.05$), ** statistically significant ($p<0.01$), *** statistically significant ($p<0.001$), **** statistically significant ($p<0.0001$).

Data availability

All relevant data are available from the authors upon reasonable request.

Results

Enhanced PARPi sensitivity in IDH2-mutant AML *in vivo*

Our earlier work on the oncometabolite 2HG suggested that the HR defect and resultant PARPi sensitivity would be tumor agnostic [19–21].

To determine whether PARPi would be efficacious in primary human MDS/AML within the context of their clonal complexity and variable co-mutational patterns, we generated a panel of IDH1/2-mutant and matched wildtype MDS and serially transplantable AML PDXs in cytokine humanized immunodeficient MISTRG mice (Table 1 and Supplementary Fig. S1A). MISTRG mice express physiologic levels of human cytokines (M-CSF$^{h/h}$, IL-3/GM-CSF$^{h/h}$ and hTPO$^{h/h}$) on the RAG2$^{-/-}$ γc$^{-/-}$ background with additional humanization

Author Manuscript Author Manuscript Author Manuscript Author Manuscript

of the CD47 receptor hSIRPα [26, 36]; they support the engraftment, maintenance, and differentiation of AML and other myeloid malignancies [24, 37]. 12–16 weeks post transplantation we confirmed primary engraftment levels of human $CD45^+$ ($huCD45^+$) AML in MISTRG mice (Supplementary Fig. S1B, C) and generated secondary recipients for drug administration as described previously [24]. Eight to twelve weeks after secondary transplantation, MISTRG mice engrafted with newly diagnosed (Y566, Y577) or relapsed/refractory (Y747) $IDH2^{R140Q}$ human AML were assigned to either vehicle or olaparib based on similar engraftment levels determined by BM aspiration and dosed intraperitoneally with vehicle or olaparib (100mg/kg) 6 days a week for 3 weeks. While in vehicle treated mice leukemia burden (Fig. 1A–C) and 2HG levels in plasma (Fig. 1D) rose sharply, especially for Y577 and Y747, engraftment and 2HG levels in olaparib treated mice remained stable or fell compared to pre-treatment levels (Fig. 1A–D and Supplementary figure S1D–F). Representative histologic assessment of $huCD45^+$ engraftment confirmed the olaparib effect on BM leukemic burden (Fig. 1E). Increased $\gamma H2AX^+$ huCD45 cells in bone marrow confirmed that olaparib induced DNA damage in IDH mutant cells (Fig. 1F). To assure that olaparib toxicity against human AML was specific to IDH mutant AML, we engrafted MISTRG mice with IDH wildtype AML and treated mice as before with vehicle or olaparib (100mg/kg) 6 days a week for 3 weeks. In MISTRG mice engrafted with IDH wildtype AML (Y689, Y406, and Y456) olaparib administration showed no benefit when compared to vehicle regardless of mutational composition, with significantly increased PB and BM tumor burden compared to pre-treatment bone marrow aspiration levels (Supplementary Fig. S2A–C).

The IDH^m inhibitors enasidenib and ivosidenib are known to induce differentiation of leukemic blasts, and we have previously been able to recapitulate the differentiation effect in IDH2 mutant MDS in MISTRG mice [24]. Unlike IDH^mi, olaparib exhibits direct toxicity on IDH mutant cells secondary to the 2HG-induced BRCAness and dependence on PARP-mediated DNA repair[9, 38, 39]. Consistent with this mechanism, olaparib did not alter lineage representation (Supplementary Fig. S3A) but significantly reduced the population of $huCD45^+Lin^-CD34^+CD38^-$ cells, previously shown to be enriched for LICs [40, 41] (Fig. 1G and Supplementary Fig. S3B). To validate that functional LIC were targeted by PARPi, we transplanted equal numbers of $huCD45^+$ BM cells from vehicle or olaparib treated mice into tertiary recipient mice (Supplementary Fig. S3C). 16 weeks after transplantation of olaparib versus vehicle treated BM, we quantitated engraftment levels in recipient mice as readout of olaparib toxicity against LIC in treated donor mice. Overall $huCD45^+$ AML engraftment levels and LICs were significantly lower in the recipients of olaparib- compared to vehicle-treated BM cells (Fig. 1H and Supplementary Fig. S3D, E and Fig. 1I, respectively), suggesting that olaparib exerted direct toxicity on LICs. These findings held true in mice engrafted with a $IDH2^{R140Q}$-mutant AML (Y747) relapsed after chemotherapy. Similarly, $huCD45^+Lin^-CD34^+CD38^-$ LICs were significantly reduced in BM of olaparib compared to vehicle treated mice (Fig. 1J) again translating into reduced leukemia burden in tertiary recipients (Fig. 1K, L and Supplementary Fig. S3F–H).

In summary, our data confirm the effectiveness of the PARPi olaparib *in vivo* specifically against $IDH2^{R140Q}$, but not IDH^{WT} AML, regardless of co-mutational pattern with toxicity against LICs.

Author Manuscript Author Manuscript Author Manuscript Author Manuscript

Olaparib-induced toxicity is preserved in IDH^{m}i-resistant IDH2-mutant AML

IDH^{m}i rarely effect cure and ultimately patients relapse with restoration of 2HG levels suggesting an oncometabolite dependence of IDH mutant AML [15–18]. We therefore sought to test whether PARPi will be effective in enasidenib-resistant IDH2-mutant AML. We first resorted to a syngeneic mouse model of AML relying on co-mutation of Flt3 with an internal tandem duplication (ITD) (Flt3^{ITD}) and of IDH2^{R140Q}. Polyinosinic: polycytidylic acid [poly (I:C)] induced activation of Mx1 promoter-driven Cre recombinase (M) results in heterozygous expression of IDH2^{R140Q} (I2) in the background of constitutive Flt3^{ITD} (F) expression and mice develop a transplantable (MFI2) leukemia as previously described [25]. To test olaparib *in vitro* in colony forming assays we established that olaparib at 1.25μM was non-toxic to IDH wildtype cells while effectively reducing colony formation in IDH2^{R140Q} mutant cells (Supplementary Fig. S4A). We generated enasidenib-resistant murine AML by transduction of MFI2 AML with lentiviral vectors expressing IDH2 carrying second site mutations Q316E or I319M, previously reported to confer enasidenib resistance in patients [18]. Lentivirally transduced MFI2 AML expressing IDH2^{I319M}, IDH2^{Q316E} or IDH2^{WT} were then subjected to serial colony formation *in vitro* in the presence of vehicle, enasidenib (50nM), or olaparib (1.25μM). Enasidenib inhibited serial replating capacity of cells expressing IDH2$^{R140/WT}$ at the third replating (CFU3) as previously shown, while the Q316E and I319M mutations conferred resistance to enasidenib but not to olaparib (Fig. 2A). These data suggest that restoration of 2HG may be sufficient to confer sensitivity to PARPi. While second site mutations have been identified only in a minority of patients [18], restoration of aberrant 2HG production is found in a significant subset of IDH^{m}i resistant patients, suggesting that PARP inhibition may be more widely applicable to mutant IDH inhibitor-resistant AML [14, 16].

We therefore investigated the olaparib response in enasidenib-resistant IDH2^{R140Q} AML from 2 patients treated at our institution. The first patient presented with newly diagnosed, intermediate-risk AML with inversion 8 (inv (8)), with an elevated WBC of 42×10^3/μl with 48% blasts in BM and 10% blasts in PB (Fig. 2B, C). Targeted next generation sequencing (NGS) of bone marrow cells at time of diagnosis revealed an IDH2^{R140Q} mutation along with mutations in SRSF2, JAK2, and ASXL1 (Table 1). The patient received azacitidine and enasidenib, which induced a significant reduction in WBC count and blast percentage (Fig. 2B, C). After almost 12 months of continuous treatment with enasidenib, the patient relapsed with rapid rise in the WBC with leukemic blast predominance (Fig. 2B, C), which preceded the patient's death. Resequencing of the mutant AML did not identify the mechanism of acquired resistance neither in the clinical targeted panel (Table 1) nor using a comprehensive AML targeted panel (Supplementary Table S1). We transplanted MISTRG mice with BM and PB mononuclear cells banked at the time of diagnosis (Y1597) and at time of relapse on enasidenib (Y2260) (Table 1 and Fig. 2B, C). Both diagnosis and relapsed AML engrafted MISTRG mice had elevated 2HG levels (Supplementary Fig. S4B, C). Secondary recipient mice were treated with vehicle, olaparib or enasidenib (40mg/kg via oral gavage) for 6 days per week for 3 weeks. While both enasidenib and olaparib effectively reduced engraftment and plasma 2HG levels in mice engrafted with the new AML diagnosis sample (Y1597), enasidenib failed to limit proliferation of the relapsed AML (Y2260) with significant rise in disease burden during the treatment course (Fig. 2D, E and Supplementary

Author Manuscript Author Manuscript Author Manuscript Author Manuscript

Fig. S4B–H). Olaparib on the other hand significantly inhibited leukemic progression compared to enasidenib (Fig. 2D, E and Supplementary Fig. S4C–H). Moreover, olaparib significantly reduced $Lin^{-}CD45^{+}CD34^{+}CD38^{-}$ LICs in both diagnosis (enasidenib-naïve) and enasidenib-resistant AML compared to vehicle and enasidenib, confirming effectiveness of olaparib against LICs (Fig. 2F, G).

Persistent sensitivity to olaparib despite acquisition of resistance to $IDH^{m}i$ was also evident in a second patient with relapsed AML (Fig. 3A, B) with $IDH2^{R140Q}$ and RUNX1 mutations (Table 1). While the patient's AML was sensitive to both enasidenib and olaparib prior to treatment with enasidenib (Y1550, Fig. 3C), after progression of disease on enasidenib, olaparib but not enasidenib effectively limited leukemic cell expansion in MISTRG (Y1840, Fig. 3D). Both enasidenib and olaparib significantly inhibited $Lin^{-}CD45^{+}CD34^{+}CD38^{-}$ LICs in the enasidenib-naïve AML engrafted mice (Y1550, Fig. 3E) while only olaparib significantly reduced LICs in the enasidenib-resistant AML engrafted mice (Y1840, Fig. 3F).

Collectively, these data show that PARP inhibition is effective in $IDH^{m}i$ resistant AML and may offer a novel treatment approach for patients with relapsed AML.

PARP sensitivity is IDH isoform- and disease-agnostic

AML and MDS carry mutations at two hotspot sites in IDH2 and in IDH1and different mutations may have in part distinct oncogenic mechanisms [42]. We therefore tested whether susceptibility to PARP inhibition was indeed independent of the mutant IDH isoform and whether PARPi could be effective in patients with MDS. We transplanted MISTRG mice with one newly diagnosed (Y276) and one relapsed/refractory secondary (Y493) $IDH1^{R132K}$ -mutant AML sample (Table 1 and Supplementary Fig. S5A). Olaparib effectively treated both $IDH1^{R132K}$ -mutant AMLs compared to vehicle (Fig. 4A, B) and despite prior exposure of Y493 to an IDH1 inhibitor (Fig. 4C, D). Olaparib administration reduced the $huCD45^{+}lin^{-}CD34^{+}CD38^{-}$ LIC population compared to vehicle treatment in both AMLs (Supplementary Fig. S5B, C) as shown for IDH2 mutant AML. Overall, these results demonstrated that olaparib monotherapy was also active against IDH1-mutant AML and thus isoform- agnostic.

Lastly, to determine whether PARP inhibition is a relevant therapy for IDH-mutant MDS, we transplanted MISTRG mice with $CD34^{+}$ cells from two patients with IDH2 mutant MDS, namely $IDH2^{R140Q}$-mutant MDS-excess blast (EB) 1 (Y1952) and EB2 (Y1365) (Table 1). Primary engrafted mice were assigned to treatment groups based on pre-treatment marrow engraftment and treated with vehicle, enasidenib or olaparib for 21 days. Enasidenib and Olaparib showed efficacy in both MDS samples with reduction in $huCD45^{+}$ engraftment in both BM and PB (Fig. 4E–F and Supplementary Fig. S5D–E) and with significant reduction in the $huCD45^{+}Lin^{-}CD38^{-}CD34^{+}$ LIC populations (Supplementary Fig. S5F–G).

Collectively, our data showed the effectiveness of the synthetic lethality-mediated approach as a novel alternative therapeutic strategy in IDH2-mutant MDS.

Author Manuscript Author Manuscript Author Manuscript Author Manuscript

Discussion

There is significant need for improvement for patients with relapsed/ refractory AML and MDS despite the availability of IDH inhibitors, which have modest and transient effectiveness. Both primary and acquired resistance mechanisms to IDH inhibitors have been identified [15–18]. Primary resistance has been highly associated with the presence of NRAS, KRAS and MAPK pathway mutations, and increased incidence of relapse has been linked to higher mutational burden [12, 14, 43]. In addition, adaptive resistance develops through the acquisition of second site mutations or via isoform switching or yet unknown mechanisms, but almost invariably aberrant 2HG levels are restored [18]. Post-resistance treatments are thus critical to prolong patients' lives.

Recent advances in the understanding of metabolic vulnerabilities induced by IDH mutations have led to the identification of an alternative strategy to leverage the concept of synthetic lethality associated with the impaired HR conferred by 2HG [44]. We here validated the efficacy of PARPi exploiting the 2HG-induced BRCAness defect in primary AML and MDS samples *in vivo* building upon our and others' prior *in vitro* studies and our previously reported highly efficient MDS/AML PDX model [19, 22, 24].

Cytokine humanized MISTRG mice express physiological levels of human cytokines instead of their murine counterparts and have overcome many challenges in modeling myeloid malignancies [36, 45]. Accordingly, our group previously reported MISTRG as an advanced and highly efficient model of MDS that faithfully replicates the intra- and inter-disease heterogeneity, the dysplastic morphology, and the mutational profile and clonal complexity [24]. We leveraged the MISTRG model to test whether PARP inhibition would be effective against a variety of IDH mutant AML, AML resistant to IDH^{m}i, and against IDH mutant MDS. Olaparib treatment demonstrated antileukemic efficacy irrespective of co-occuring mutations as long as cells carried IDH1/2 mutations, while olaparib was ineffective against IDH1/2 wildtype AML. In addition, olaparib demonstrated toxicity against phenotypic and functional LICs, a rare subpopulation of leukemic cells that possess stem cell properties, including leukemia initiation and self-renewal, as evident by engraftment in immunodeficient mice as shown here, and drug resistance [46, 47].

Our data also demonstrates that PARP inhibition could represent a new choice for patients with primary refractoriness to IDH inhibitors or for those who relapse on IDH1/2 inhibitor treatment irrespective of tumor type [19]. The PRIME clinical trial (NCI10264) is currently testing the overall response of IDH1/2-mutant relapsed/refractory AML and MDS to PARP inhibitor monotherapy, which further underlines the clinical relevance of the results presented here. Future studies combining PARP inhibitors with other DNA damaging agents or agents with complementary activity will be important to leverage this mechanism against MDS/AML as monotherapy rarely results in cure.

Collectively, our data provide critical insights which support the pursuit of PARP inhibition as a promising therapeutic tool for IDH mutated MDS/AML patients.

Author Manuscript Author Manuscript Author Manuscript Author Manuscript

Supplementary Material

Refer to Web version on PubMed Central for supplementary material.

Acknowledgements

We thank Yale Pathology Tissue Services especially A. Brooks for research histology services. We thank Yale Animal Resources Center, especially P. Ranney, J. Fonck for animal care. We thank Yale Flow Cytometry Core, especially Lesley Divine, Diane Trotta and Chao Wang for flow cytometry analysis. We thank our patients for donating blood and bone marrow to research. This study was supported in part by the NIH/NIDDK R01DK102792 (to S.H.), The Frederick A. Deluca Foundation and the Vera and Joseph Dresner Foundation (to S.H.), the Howard Hughes Medical Institute (to R.A.F), General Program of the National Natural Science Foundation of China (Grant No.82170137, to Y.S.), and the Leukemia and Lymphoma Society and the NIH/NCI R01CA266604 (to S.H. and R.S.B.). Y.S. was supported by the General Program of the National Natural Science Foundation of China (Grant No.82170137). X.F. was supported by the Young Scientists Fund of the National Natural Science Foundation of China (Grant No. 81801588). Y.G. was supported by the American Society of Hematology Scholar Award. This study was supported by the Animal Modeling Core, Pilot and Feasibility Program of the Yale Cooperative Center of Excellence in Hematology (NIDDK U54DK106857).

Disclosure of conflicts of interest

Zeidan: A.M.Z. received research funding from *Celgene/BMS*, *Abbvie*, *Astex*, *Pfizer*, *Medimmune/AstraZeneca*, *Boehringer-Ingelheim*, *Trovagene/Cardiff Oncology*, *Incyte*, *Takeda*, *Novartis*, *Aprea*, *Amgen*, and *ADC Therapeutics*. A.M.Z participated in advisory boards, had a consultancy with, and/or received honoraria from *AbbVie*, *Otsuka*, *Pfizer*, *Celgene/BMS*, *Jazz*, *Incyte*, *Agios*, *Boehringer-Ingelheim*, *Novartis*, *Acceleron*, *Astellas*, *Daiichi Sankyo, Cardinal Health*, *Taiho*, *Seattle Genetics*, *BeyondSpring*, *Trovagene/Cardiff Oncology*, *Takeda*, *Ionis*, *Amgen*, *Tyme*, *Aprea*, *Kura*, *Janssen*, *Gilead*, and *Epizyme*. A.M.Z received travel support for meetings from *Pfizer*, *Novartis*, and *Trovagene*.

Flavell: *Zai labs:* Consultancy; *GSK:* Consultancy.

Prebet: *Boehringer Ingelheim:* Research Funding; *Novartis:* Honoraria; *Pfizer:* Honoraria; *Agios:* Consultancy, Research Funding; *Jazz Pharmaceuticals:* Consultancy, Honoraria, Research Funding; *Genentech*: Consultancy; *Tetraphase*: Consultancy; *Bristol-Myers Squibb*: Honoraria, Research Funding.

Bindra: *Cybrexa Therapeutics*: Consultancy, Equity Ownership. *Athena Therapeutics:* Equity Ownership.

Halene: *Forma Therapeutics:* Consultancy

References

1. Showalter MR, Hatakeyama J, Cajka T, VanderVorst K, Carraway KL, Fiehn O, et al. Replication Study: The common feature of leukemia-associated IDH1 and IDH2 mutations is a neomorphic enzyme activity converting alpha-ketoglutarate to 2-hydroxyglutarate. Elife 2017 Jun 27; 6.
2. Winer ES, Stone RM. Novel therapy in Acute myeloid leukemia (AML): moving toward targeted approaches. Ther Adv Hematol 2019; 10: 2040620719860645.
3. Clark O, Yen K, Mellinghoff IK. Molecular Pathways: Isocitrate Dehydrogenase Mutations in Cancer. Clin Cancer Res 2016 Apr 15; 22(8): 1837–1842. [PubMed: 26819452]
4. DiNardo CD, Jabbour E, Ravandi F, Takahashi K, Daver N, Routbort M, et al. IDH1 and IDH2 mutations in myelodysplastic syndromes and role in disease progression. Leukemia 2016 Apr; 30(4): 980–984. [PubMed: 26228814]
5. Losman JA, Kaelin WG Jr., What a difference a hydroxyl makes: mutant IDH, (R)-2-hydroxyglutarate, and cancer. Genes Dev 2013 Apr 15; 27(8): 836–852. [PubMed: 23630074]
6. Rakheja D, Medeiros LJ, Bevan S, Chen W. The emerging role of d-2-hydroxyglutarate as an oncometabolite in hematolymphoid and central nervous system neoplasms. Front Oncol 2013; 3: 169. [PubMed: 23847760]
7. Xu W, Yang H, Liu Y, Yang Y, Wang P, Kim SH, et al. Oncometabolite 2-hydroxyglutarate is a competitive inhibitor of alpha-ketoglutarate-dependent dioxygenases. Cancer Cell 2011 Jan 18; 19(1): 17–30. [PubMed: 21251613]

Author Manuscript Author Manuscript Author Manuscript Author Manuscript

8. Molenaar RJ, Radivoyevitch T, Maciejewski JP, van Noorden CJ, Bleeker FE. The driver and passenger effects of isocitrate dehydrogenase 1 and 2 mutations in oncogenesis and survival prolongation. Biochim Biophys Acta 2014 Dec; 1846(2): 326–341. [PubMed: 24880135]
9. Wang Y, Wild AT, Turcan S, Wu WH, Sigel C, Klimstra DS, et al. Targeting therapeutic vulnerabilities with PARP inhibition and radiation in IDH-mutant gliomas and cholangiocarcinomas. Sci Adv 2020 Apr; 6(17): eaaz3221.
10. Norsworthy KJ, Luo L, Hsu V, Gudi R, Dorff SE, Przepiorka D, et al. FDA Approval Summary: Ivosidenib for Relapsed or Refractory Acute Myeloid Leukemia with an Isocitrate Dehydrogenase-1 Mutation. Clin Cancer Res 2019 Jun 1; 25(11): 3205–3209. [PubMed: 30692099]
11. Kim ES. Enasidenib: First Global Approval. Drugs 2017 Oct; 77(15): 1705–1711. [PubMed: 28879540]
12. Liu X, Gong Y. Isocitrate dehydrogenase inhibitors in acute myeloid leukemia. Biomark Res 2019; 7: 22. [PubMed: 31660152]
13. Upadhyay VA, Brunner AM, Fathi AT. Isocitrate dehydrogenase (IDH) inhibition as treatment of myeloid malignancies: Progress and future directions. Pharmacol Ther 2017 Sep; 177: 123–128. [PubMed: 28315358]
14. Amatangelo MD, Quek L, Shih A, Stein EM, Roshal M, David MD, et al. Enasidenib induces acute myeloid leukemia cell differentiation to promote clinical response. Blood 2017; 130(6): 732–741. [PubMed: 28588019]
15. Choe S, Wang H, DiNardo CD, Stein EM, de Botton S, Roboz GJ, et al. Molecular mechanisms mediating relapse following ivosidenib monotherapy in IDH1-mutant relapsed or refractory AML. Blood Adv 2020 May 12; 4(9): 1894–1905. [PubMed: 32380538]
16. Quek L, David MD, Kennedy A, Metzner M, Amatangelo M, Shih A, et al. Clonal heterogeneity of acute myeloid leukemia treated with the IDH2 inhibitor enasidenib. Nat Med 2018 Aug; 24(8): 1167–1177. [PubMed: 30013198]
17. Harding JJ, Lowery MA, Shih AH, Schvartzman JM, Hou S, Famulare C, et al. Isoform Switching as a Mechanism of Acquired Resistance to Mutant Isocitrate Dehydrogenase Inhibition. Cancer Discov 2018 Dec; 8(12): 1540–1547. [PubMed: 30355724]
18. Intlekofer AM, Shih AH, Wang B, Nazir A, Rustenburg AS, Albanese SK, et al. Acquired resistance to IDH inhibition through trans or cis dimer-interface mutations. Nature 2018 Jul; 559(7712): 125–129. [PubMed: 29950729]
19. Sulkowski PL, Corso CD, Robinson ND, Scanlon SE, Purshouse KR, Bai H, et al. 2-Hydroxyglutarate produced by neomorphic IDH mutations suppresses homologous recombination and induces PARP inhibitor sensitivity. Sci Transl Med 2017 Feb 1; 9(375).
20. Sulkowski PL, Oeck S, Dow J, Economos NG, Mirfakhraie L, Liu Y, et al. Oncometabolites suppress DNA repair by disrupting local chromatin signalling. Nature 2020 Jun; 582(7813): 586–591. [PubMed: 32494005]
21. Sulkowski PL, Sundaram RK, Oeck S, Corso CD, Liu Y, Noorbakhsh S, et al. Krebs-cycle-deficient hereditary cancer syndromes are defined by defects in homologous-recombination DNA repair. Nat Genet 2018 Aug; 50(8): 1086–1092. [PubMed: 30013182]
22. Molenaar RJ, Radivoyevitch T, Nagata Y, Khurshed M, Przychodzen B, Makishima H, et al. IDH1/2 Mutations Sensitize Acute Myeloid Leukemia to PARP Inhibition and This Is Reversed by IDH1/2-Mutant Inhibitors. Clin Cancer Res 2018 Apr 1; 24(7): 1705–1715. [PubMed: 29339439]
23. Philip B, Yu DX, Silvis MR, Shin CH, Robinson JP, Robinson GL, et al. Mutant IDH1 Promotes Glioma Formation In Vivo. Cell Rep 2018 May 1; 23(5): 1553–1564. [PubMed: 29719265]
24. Song Y, Rongvaux A, Taylor A, Jiang T, Tebaldi T, Balasubramanian K, et al. A highly efficient and faithful MDS patient-derived xenotransplantation model for pre-clinical studies. Nat Commun 2019 Jan 21; 10(1): 366. [PubMed: 30664659]
25. Shih AH, Meydan C, Shank K, Garrett-Bakelman FE, Ward PS, Intlekofer AM, et al. Combination Targeted Therapy to Disrupt Aberrant Oncogenic Signaling and Reverse Epigenetic Dysfunction in IDH2- and TET2-Mutant Acute Myeloid Leukemia. Cancer Discov 2017 May; 7(5): 494–505. [PubMed: 28193779]

Author Manuscript Author Manuscript Author Manuscript Author Manuscript

26. Rongvaux A, Willinger T, Martinek J, Strowig T, Gearty SV, Teichmann LL, et al. Development and function of human innate immune cells in a humanized mouse model. Nat Biotechnol 2014 Apr; 32(4): 364–372. [PubMed: 24633240]
27. Wingett SW, Andrews S. FastQ Screen: A tool for multi-genome mapping and quality control. F1000Res 2018; 7: 1338. [PubMed: 30254741]
28. Li H, Durbin R. Fast and accurate long-read alignment with Burrows-Wheeler transform. Bioinformatics 2010 Mar 1; 26(5): 589–595. [PubMed: 20080505]
29. Li H, Handsaker B, Wysoker A, Fennell T, Ruan J, Homer N, et al. The Sequence Alignment/Map format and SAMtools. Bioinformatics 2009 Aug 15; 25(16): 2078–2079. [PubMed: 19505943]
30. Quinlan AR, Hall IM. BEDTools: a flexible suite of utilities for comparing genomic features. Bioinformatics 2010 Mar 15; 26(6): 841–842. [PubMed: 20110278]
31. Benjamin D, Sato T, Cibulskis K, Getz G, Stewart C, Lichtenstein L. Calling Somatic SNVs and Indels with Mutect2. bioRxiv 2019: 861054.
32. Wang K, Li M, Hakonarson H. ANNOVAR: functional annotation of genetic variants from high-throughput sequencing data. Nucleic Acids Res 2010 Sep; 38(16): e164. [PubMed: 20601685]
33. Shihab HA, Gough J, Cooper DN, Stenson PD, Barker GL, Edwards KJ, et al. Predicting the functional, molecular, and phenotypic consequences of amino acid substitutions using hidden Markov models. Hum Mutat 2013 Jan; 34(1): 57–65. [PubMed: 23033316]
34. Tate JG, Bamford S, Jubb HC, Sondka Z, Beare DM, Bindal N, et al. COSMIC: the Catalogue Of Somatic Mutations In Cancer. Nucleic Acids Res 2019 Jan 8; 47(D1): D941–D947. [PubMed: 30371878]
35. Robinson JT, Thorvaldsdottir H, Wenger AM, Zehir A, Mesirov JP. Variant Review with the Integrative Genomics Viewer. Cancer Res 2017 Nov 1; 77(21): e31–e34. [PubMed: 29092934]
36. Saito Y, Ellegast JM, Rafiei A, Song Y, Kull D, Heikenwalder M, et al. Peripheral blood CD34(+) cells efficiently engraft human cytokine knock-in mice. Blood 2016 Oct 6; 128(14): 1829–1833. [PubMed: 27543436]
37. Ellegast JM, Rauch PJ, Kovtonyuk LV, Muller R, Wagner U, Saito Y, et al. inv(16) and NPM1mut AMLs engraft human cytokine knock-in mice. Blood 2016 Oct 27; 128(17): 2130–2134. [PubMed: 27581357]
38. Lu Y, Kwintkiewicz J, Liu Y, Tech K, Frady LN, Su YT, et al. Chemosensitivity of IDH1-Mutated Gliomas Due to an Impairment in PARP1-Mediated DNA Repair. Cancer Res 2017 Apr 1; 77(7): 1709–1718. [PubMed: 28202508]
39. Tateishi K, Higuchi F, Miller JJ, Koerner MVA, Lelic N, Shankar GM, et al. The Alkylating Chemotherapeutic Temozolomide Induces Metabolic Stress in IDH1-Mutant Cancers and Potentiates NAD(+) Depletion-Mediated Cytotoxicity. Cancer Res 2017 Aug 1; 77(15): 4102–4115. [PubMed: 28625978]
40. Lapidot T, Sirard C, Vormoor J, Murdoch B, Hoang T, Caceres-Cortes J, et al. A cell initiating human acute myeloid leukaemia after transplantation into SCID mice. Nature 1994 Feb 17; 367(6464): 645–648. [PubMed: 7509044]
41. Bonnet D, Dick JE. Human acute myeloid leukemia is organized as a hierarchy that originates from a primitive hematopoietic cell. Nat Med 1997 Jul; 3(7): 730–737. [PubMed: 9212098]
42. Wang HY, Tang K, Liang TY, Zhang WZ, Li JY, Wang W, et al. The comparison of clinical and biological characteristics between IDH1 and IDH2 mutations in gliomas. J Exp Clin Cancer Res 2016 May 31; 35: 86. [PubMed: 27245697]
43. Stein EM, DiNardo CD, Fathi AT, Pollyea DA, Stone RM, Altman JK, et al. Molecular remission and response patterns in patients with mutant-IDH2 acute myeloid leukemia treated with enasidenib. Blood 2019 Feb 14; 133(7): 676–687. [PubMed: 30510081]
44. Madala HR, Punganuru SR, Arutla V, Misra S, Thomas TJ, Srivenugopal KS. Beyond Brooding on Oncometabolic Havoc in IDH-Mutant Gliomas and AML: Current and Future Therapeutic Strategies. Cancers (Basel) 2018 Feb 11; 10(2).
45. Rongvaux A, Takizawa H, Strowig T, Willinger T, Eynon EE, Flavell RA, et al. Human hemato-lymphoid system mice: current use and future potential for medicine. Annu Rev Immunol 2013; 31: 635–674. [PubMed: 23330956]

Author Manuscript Author Manuscript Author Manuscript Author Manuscript

46. Dick JE. Stem cell concepts renew cancer research. Blood 2008 Dec 15; 112(13): 4793–4807. [PubMed: 19064739]

47. Saito Y, Uchida N, Tanaka S, Suzuki N, Tomizawa-Murasawa M, Sone A, et al. Induction of cell cycle entry eliminates human leukemia stem cells in a mouse model of AML. Nat Biotechnol 2010 Mar; 28(3): 275–280. [PubMed: 20160717]

Author Manuscript Author Manuscript Author Manuscript Author Manuscript

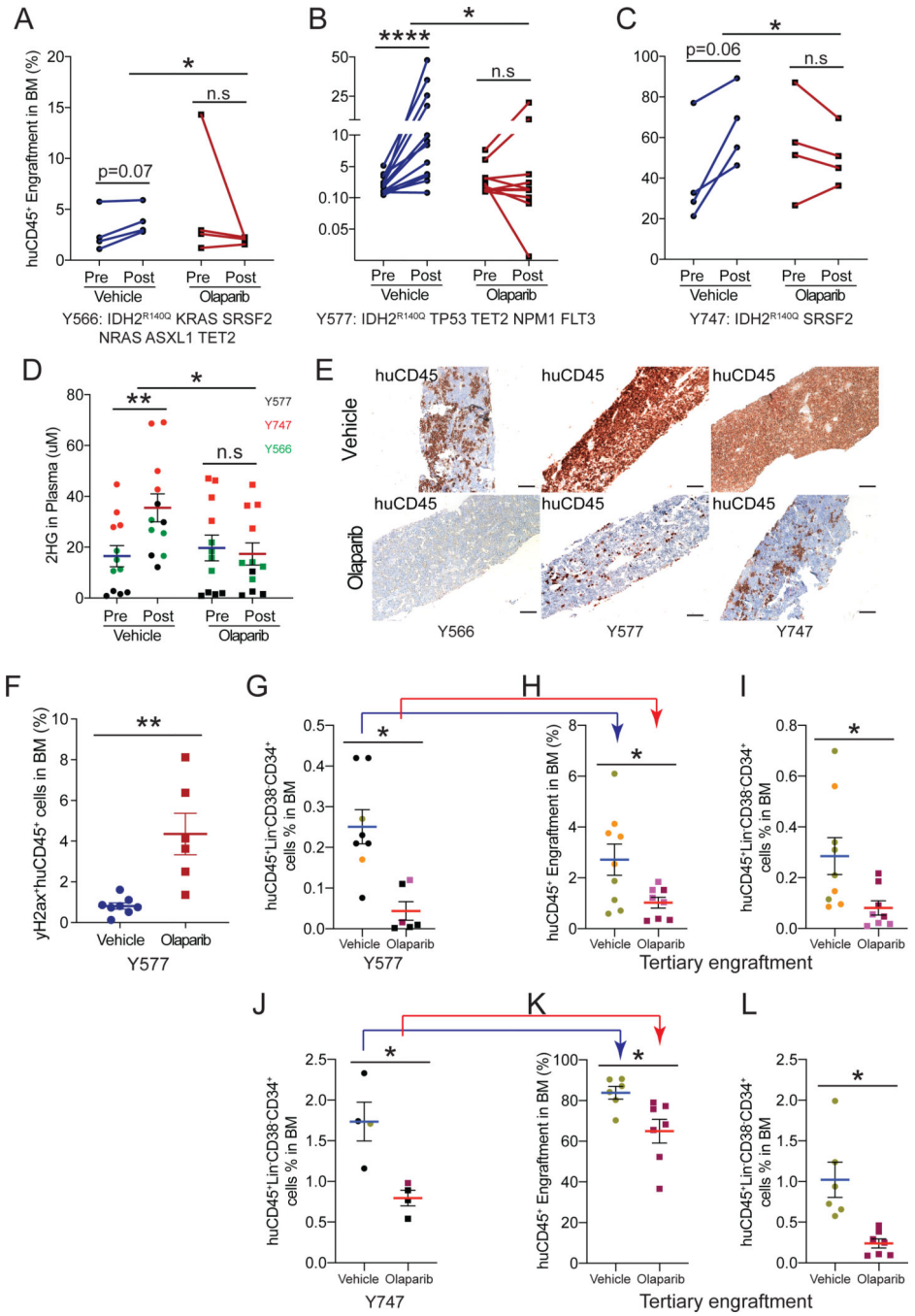

Fig 1. Olaparib targets IDH2-mutant AML blasts and leukemia initiating cells *in vivo*.

A-E, Secondary MISTRG recipients engrafted with BM cells collected from primary MISTRG mice, transplanted with three different IDH2^{R140Q} AML patient samples. Secondary mice were treated with either vehicle or olaparib (100mg/Kg) 6 days a week for 21 days. **A-C**, Pre- and post-treatment comparison of human CD45^{+} engraftment levels in BM of secondary treated mice. **A**, Y566 (vehicle, n=4, olaparib, n= 4); **B**, Y577 (vehicle n= 12, olaparib n= 8); **C**, Y747 (vehicle n= 4, olaparib n= 4). Individual mice are represented by matching pre-post symbols; *P* values were determined by ratio paired t test

Author Manuscript Author Manuscript Author Manuscript Author Manuscript

for pre-post treatment within groups and by Mann-Whitney test for comparison between treatment groups; n.s. not significant, *$p < 0.05$, ****$p < 0.0001$). **D,** Plasma concentrations of D-2-HG in pre-versus post administration of vehicle or olaparib. Individual mice are represented by symbols with mean ± S.E.M.; *P* values were determined by Mann–Whitney test; n.s. not significant, *$p < 0.05$, **$p < 0.01$. **E,** Immunohistochemistry (IHC) staining for hCD45 of BM of vehicle (top panel) and olaparib (lower panel) treated mice (scale bars 100 μm, original magnification 10x). **F**, Comparison of γH2AX^{+} huCD45 cells in bone marrow of secondary mice of Y577 treated with vehicle and olaparib (vehicle n= 8, olaparib n= 6). **G-I,** Secondary (2°) and tertiary (3°) transplantation of IDH2^{R140Q} AML (Y577). **G,** Comparison of huCD45^{+}lin^{-}huCD34^{+}CD38^{-} population in BM of vehicle (n=8) vs olaparib (n=6) treated mice. Quantification of huCD45^{+} engraftment levels (**H**) and huCD45^{+}lin^{-}huCD34^{+}CD38^{-} population (**I**) in the BM of tertiary mice engrafted with equal numbers of huCD45^{+} BM cells (5×10^{5}) of vehicle (n=9) vs. olaparib (n=8) treated mice. **J-L,** Secondary and tertiary transplantation of IDH2^{R140Q} AML (Y747). **J,** Comparison of huCD45^{+}lin^{-}huCD34^{+}CD38^{-} population in the BM of vehicle (n=4) vs olaparib (n=4) treated mice. Quantification of huCD45^{+} engraftment levels **(K)** and huCD45^{+}lin^{-}huCD34^{+}CD38^{-} population **(L)** in the BM of tertiary mice engrafted with equal numbers of huCD45^{+} BM cells (5×10^{5}) of vehicle (n=6) vs. olaparib (n=7) post-treatment mice. Individual mice are represented by symbols with means ± S.E.M.; symbols for corresponding 2° and 3° recipient mice are color coded; statistics represent Mann–Whitney test; n.s. not significant, *$p < 0.05$, **$p < 0.01$.

Author Manuscript Author Manuscript Author Manuscript Author Manuscript

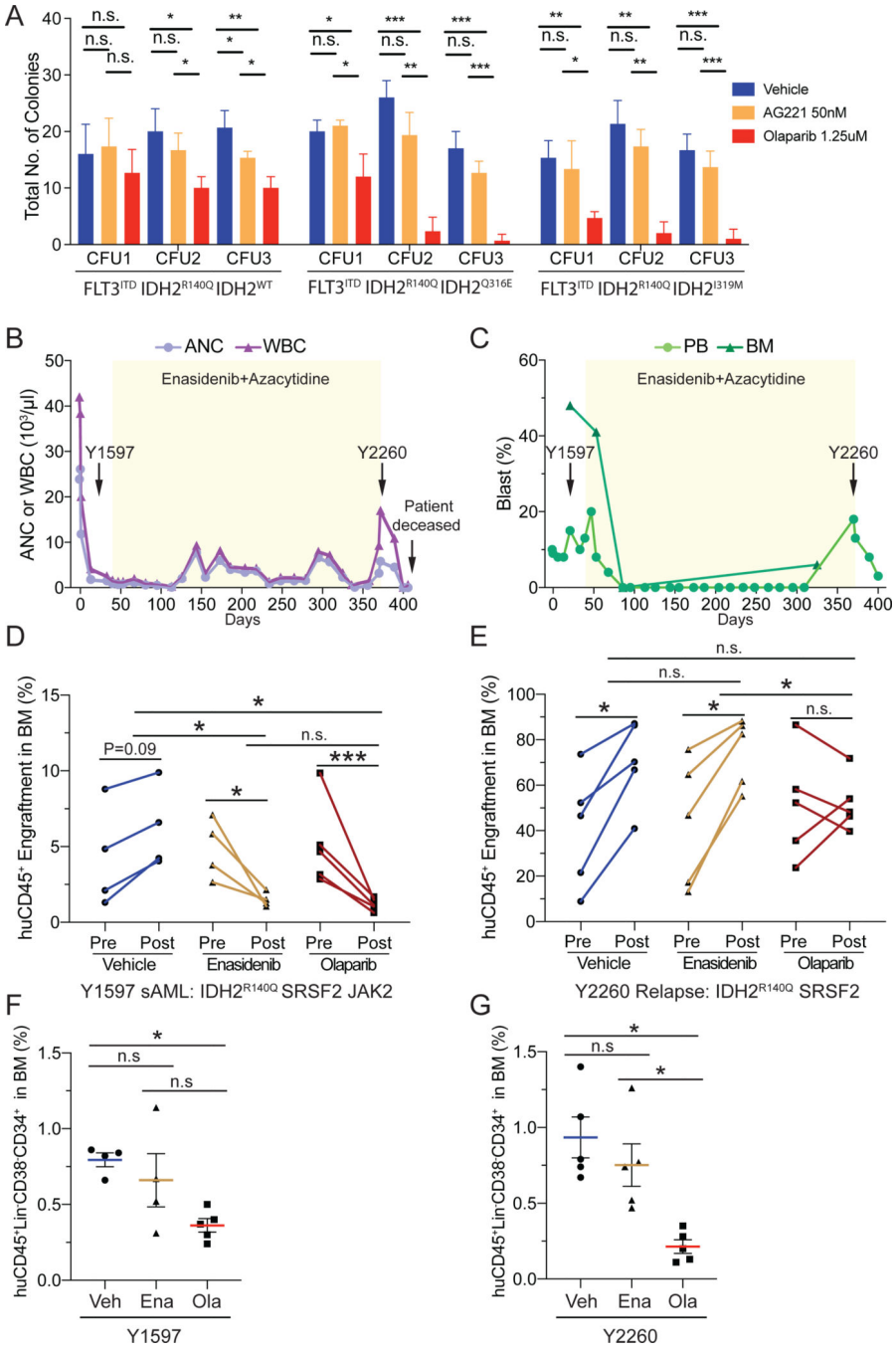

Fig 2. Enasidenib resistant AML is sensitive to olaparib administration both *in vitro* and *in vivo*.

A, Colony forming unit assay (CFU) re-plating of hematopoietic stem and progenitor cells (HSPCs) from $FLT3^{ITD}IDH2^{R140Q}$ linage depleted primary murine cells expressing IDH2 WT or Q316E or I319M *in trans* and cultured in methocult containing vehicle, AG-221 at 50nM, or olaparib at 1.25µM. Data are mean ± SEM. for triplicate (CFU1/2) culture. *P* values were determined by Mann-Whitney; $*p < 0.05$, $**p < 0.01$, $***p<0.001$. This is a representation of 2 independent experiments. **B-C**, Clinical and laboratory features for a AML patient at the time of $IDH2^{R140Q}$ AML diagnosis (Y1597) (**B**) and after

Author Manuscript Author Manuscript Author Manuscript Author Manuscript

relapse on azacytidine + enasidenib treatment (Y2260) (**C**), including blood absolute neutrophil count (ANC) and white blood cell count (WBC), and blast percentage in PB and BM. **D**, Human $CD45^+$ engraftment levels in the BM of secondary mice of (Y1597) treated with vehicle (n=4), enasidenib (n=4), or olaparib (n=5); enasidenib (40mg/kg) was administered via oral gavage and olaparib (100mg/kg) intraperitoneally for 6 days per week for 3 weeks. **E**, Human $CD45^+$ engraftment levels in the BM of secondary mice of (Y2260) treated with vehicle (n=5), enasidenib (n=5), or olaparib (n=5). Individual mice are represented by matching pre-post symbols; *P* values were determined by ratio paired t test for pre-post treatment within groups and by Mann-Whitney test for comparison between different treatment groups; n.s. not significant, $*p < 0.05$, $***p<0.001$. **F-G,** Comparison of $huCD45^+lin^-huCD34^+CD38^-$ population in BM of treated mice of Y1597 (**F**) and of Y2260 (**G**).

Author Manuscript
Author Manuscript
Author Manuscript
Author Manuscript

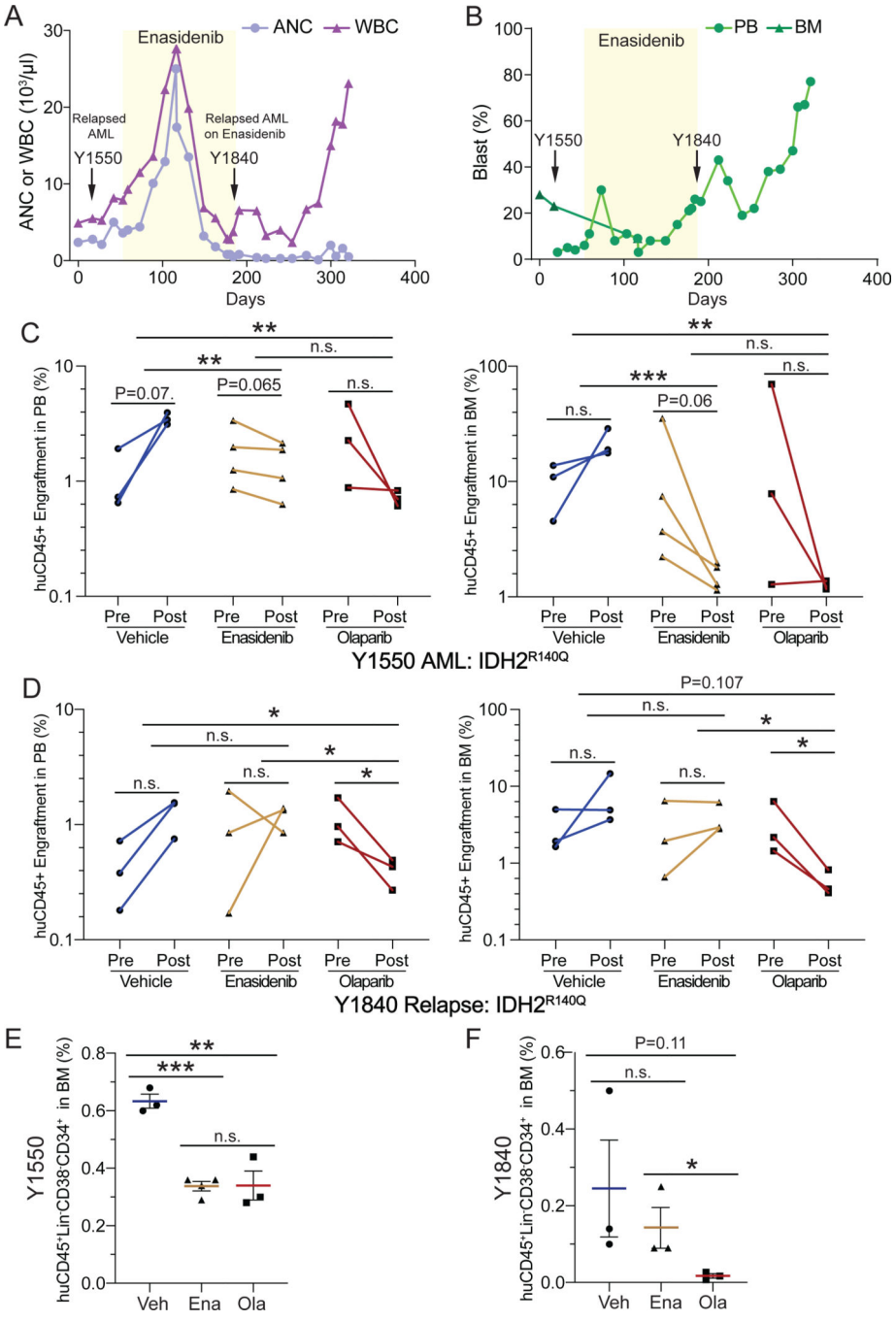

Fig 3. Olaparib remains effective in a second enasidenib-resistant IDH2-mutant AML PDX.

A-B, Clinical and laboratory features for a relapsed IDH2^{R140Q} AML patient prior to treatment with enasidenib (Y1550) (**A**) and after relapse on enasidenib treatment (Y1840) (**B**), including blood absolute neutrophil count (ANC) and white blood cell count (WBC), and blast percentage in PB and BM. **C**, Human CD45^{+} engraftment levels in the PB and BM of secondary mice of (Y1550) treated with vehicle (n=3), enasidenib (n=4), or olaparib (n=3). **D**, Human CD45^{+} engraftment levels in the PB and BM of secondary mice of (Y1840) treated with vehicle (n=3), enasidenib (n=3), or olaparib (n=3). **E-F,** Comparison

Author Manuscript Author Manuscript Author Manuscript Author Manuscript

of huCD45^{+}lin^{-}huCD34^{+}CD38^{-} population in BM of treated mice of Y1550 (**E**) and of Y1840 (**F**). Individual mice are represented by matching pre-post symbols; *P* values were determined by ratio paired t test for pre-post treatment within groups and by Mann-Whitney test for comparison between different treatment groups; n.s. not significant, *$p < 0.05$, ***$p<0.001$.

Author Manuscript Author Manuscript Author Manuscript Author Manuscript

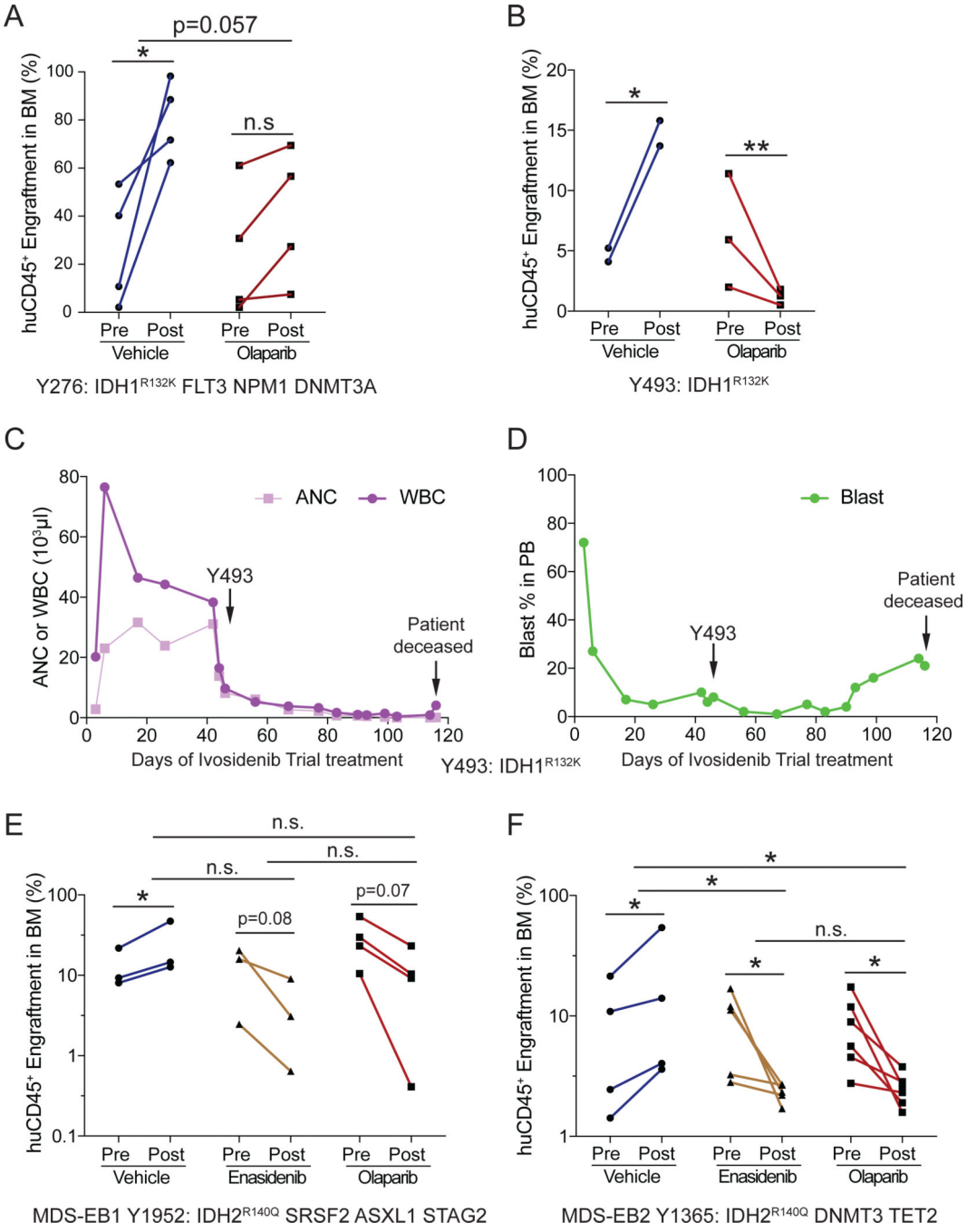

Fig 4. PARP inhibition is also effective in IDH1-mutant AML and IDH1/2-mutant MDS.

A-B, Assessment of human CD45$^+$ chimerism levels in vehicle vs olaparib treated secondary MISTRG mice engrafted with BM cells collected from primary mice transplanted with IDH1^{R132K} AML. **A**, Y276 (vehicle, n=4, olaparib, n= 4); **B**, Y493 (vehicle n= 2, olaparib n= 3). Primary patient BM CD34$^+$ HSPCs were pre-incubated with anti-CD3 antibody (OKT3) and injected intra-hepatically into newborn MISTRG mice conditioned twice with 150cGy. **C-D**, Clinical and laboratory data for a relapsed/refractory IDH1^{R132K} AML (Y493) while on ivosidenib trial treatment, including ANC, WBC, (**C**) and blast percentage

Author Manuscript Author Manuscript Author Manuscript Author Manuscript

(**D**) in PB. **E-F**, Chimerism detection of huCD45^{+} percentages in BM preceded treating the mice with either vehicle, enasidenib, or olaparib. Mice were analyzed 21 days after drug administration. **E**, Comparison of overall human CD45^{+} engraftment in BM of mice engrafted with IDH2^{R140Q} MDS-EB1 (Y1952) treated with vehicle (n=3), enasidenib (n=3), or olaparib (n=4). **F**, Comparison of overall human CD45^{+} engraftment in BM of mice engrafted with IDH2^{R140Q} MDS-EB2 (Y1365) treated with vehicle (n=4), enasidenib (n=5), or olaparib (n=6). Individual mice are represented by matching pre-post symbols; *P* values were determined by ratio paired t test for pre-post treatment within groups and by Mann-Whitney test for comparison between treatment groups; n.s. not significant, *$p < 0.05$, **$p<0.01$.

Author Manuscript Author Manuscript Author Manuscript Author Manuscript

Table 1.
Clinical characterization of the selected IDH2R140Q and IDHWT AML/MDS patients.

Patients 1–7 were IDH2^{R140Q}AML; patients 8–10 were IDH1/2^{WT}; patients 11–12 were IDH1^{R132K}, and patients 13–14 were IDH2^{R140Q}MDS. N/A, not applicable.

Patient ID	Sample type	Age	Gender	Diagnosis	Blast%	Karyotype	IDH mutation status	IDH mutation VAF	Co-occuring mutations
Y566	PB	61	M	AML arising from chronic myelomonocytic leukemia	PB:7, BM:35	47,XY,add(5)(q34),add(6)(q23),+8,−17,der(22)t(1;22)(q21;p11.2)[cp7]/46,XY[8]	IDH2^{R140Q}	42.3	NRAS, IDH2, JAK2, SRSF2
Y577	PB	26	F	New diagnosis AML with no prior chemotherapy	PB:68, BM:90	NK	IDH2^{R140Q}	38.4	NPM1
Y747	BM	62	M	Relapsed refractory AML (progressed from MDS)	PB: 28, BM:59	46,XY,der(15)t(1;15)(q12;p12)[7]/46,idem, del(20)(q11.2q13.3)[8]	IDH2^{R140Q}	47	SRSF2, TET2
Y1597	BM	77	M	New diagnosis AML	PB:15, BM:48	46,XY,del(8)(q23.2q24.13)[8]/46,XY[7]	IDH2^{R140Q}	50.1	SRSF2, JAK2, ASXL1
Y2260	PB	78	M	Relapsed AML after azacitidine+enasidenib	PB:13	46,XY,del(8)(q23.2q24.13)[8]/46,XY[7]	IDH2^{R140Q}	NA	SRSF2
Y1550	BM	75	M	Relapsed AML	PB:3, BM:23	NK	IDH2^{R140Q}	NA	SRSF2, RUNX1
Y1840	PB	75	M	Relapsed AML after enasidenib	PB:25	NK	IDH2^{R140Q}	NA	SRSF2, RUNX1
Y689	BM	63	M	New diagnosis AML, progressed from MDS after failed azacitidine therapy	PB:12, BM:13	NK	WT		SRSF2, ASXL1, CBL, NRAS, KRAS
Y406	PB	59	M	New diagnosis AML	PB:15, BM:40	46,XY,inv(3)(q21q26),del(5)(q14q34), del(13)(q13q21)[15]	WT		RUNX1
Y456	BM	46	F	AML	PB:5, BM:36	NK	WT		NPM1, WT1, FLT3^{ITD}, FLT3^{D835}
Y276	BM	39	F	New diagnosis AML on Hydrea	PB:92, BM:77	NK	IDH1^{R132K}	NA	NPM1, FLT3^{D835}
Y493	PB	59	F	Relapsed/Refractory AML from MDS- on clinical trial with IDH1 inhibitor with new anemia	PB:6, BM:30	NK	IDH1^{R132K}	NA	
Y1952	BM	86	F	MDS-EB1	BM:8	NK	IDH2^{R140Q}	47.3	SRSF2, ASXL1, STAG2
Y1365	BM	58	M	MDS-EB2	PB:3, BM:9	NK	IDH2^{R140Q}	39	DNMT3A

N/A, not applicable